Available online at www.sciencedirect.com

SCIENCE DIRECT®

Nuclear Instruments and Methods in Physics Research A 518 (2004) 188–192

NUCLEAR INSTRUMENTS & METHODS IN PHYSICS RESEARCH Section A

www.elsevier.com/locate/nima

Commissioning and first tests of the MAGIC telescope

C. Baixeras[a], D. Bastieri[b,o], C. Bigongiari[b,o], O. Blanch[c], G. Blanchot[c], R. Bock[d], T. Bretz[e], A. Chilingarian[f], J.A. Coarasa[d], E. Colombo[e], J.C. Contreras[g], D. Corti[b,o], J. Cortina[c], C. Domingo[a], E. Domingo[c], D. Ferenc[h], E. Fernández[c], J. Flix[c], V. Fonseca[g], L. Font[a], N. Galante[i,p], M. Gaug[c], M. Garczarczyk[d], J. Gebauer[d], M. Giller[j], F. Goebel[d], T. Hengstebeck[k], P. Jacone[j], O.C. de Jager[l], O. Kalekin[k], M. Kestel[e], T. Kneiske[e], A. Laille[h], M. López[g], J. López[c], E. Lorenz[d], K. Mannheim[e], M. Mariotti[b,o,*], M. Martínez[c], K. Mase[d], M. Merck[e], M. Meucci[i,p], L. Miralles[c], R. Mirzoyan[d], A. Moralejo[b,o], E. Oña Wilhelmi[g], R. Orduña[a], D. Paneque[d], R. Paoletti[i,p], D. Pascoli[b,o], N. Pavel[k], R. Pegna[i,p], L. Peruzzo[b,o], A. Piccioli[i,p], A. Roberts[a], R. Reyes[g], A. Saggion[b,o], A. Sánchez[a], P. Sartori[b,o], V. Scalzotto[b,o], T. Schweizer[c], A. Sillanpaa[m], D. Sobczynska[j], A. Stamerra[i,p], A. Stepanian[n], R. Stiehler[k], L. Takalo[m], M. Teshima[d], N. Tonello[d], A. Torres[a], N. Turini[i,p], V. Vitale[d], S. Volkov[k], R.M. Wagner[d], T. Wibig[j], W. Wittek[d]

[a] *Universitat Autònoma de Barcelona, Barcelona, Spain*
[b] *Dipartimento di Fisica, Università di Padova, Italy*
[c] *Institut de Fisica d'Altes Energies, Barcelona, Spain*
[d] *Max-Planck-Institut für Physik, München, Germany*
[e] *Universität Würzburg, Germany*
[f] *Yerevan Physics Institute, Cosmic Ray Division, Yerevan, Armenia*
[g] *Universidad Complutense, Madrid, Spain*
[h] *University of California, Davis, CA, USA*
[i] *Dipartimento di Fisica, Università di Siena, Italy*
[j] *Division of Experimental Physics, University of Lodz, Poland*
[k] *Fachbereich Physik, Universität-GH Siegen, Germany*
[l] *Space Research Unit, Potchefstroom University, South Africa*
[m] *Tuorla Observatory, Pikkiö, Finland*
[n] *Crimean Astrophysical Observatory, Nauchny Ukraine*
[o] *INFN, Sezione di Padova, Via F. Marzolo 8, Padova 35121, Italy*
[p] *INFN, Sez. Pisa, Italy*

Abstract

Major Atmospheric Gamma Imaging Cherenkov telescope is starting its operations with a set of engineering runs to tune the telescope subsystem elements to be ready for the first physics campaign. Many technical improvements have

*Corresponding author. Address for correspondence: INFN, Sezione di Padova, Via F. Marzolo 8, Padova 35121, Italy.
E-mail address: mariotti@pd.infn.it (M. Mariotti).

doi:10.1016/j.nima.2003.10.057

been developed and implemented in several elements of the telescope to reach the lowest energy threshold ever obtained by an Imaging Atmospheric Cherenkov Telescope. A general description of the telescope is presented. The commissioning of the telescope's elements is described and the expected performances are reviewed with the final detector set-up.

PACS: 95.55.Ka; 98.70.Rz

Keywords: Astroparticle physics; Cherenkov telescopes; Gamma ray astronomy

1. Introduction

The aim of the new generation Cherenkov telescopes is to bridge the observational energy gap between the upper limit of satellite-borne experiments, 10 GeV, and the lower limit 250 GeV, of the previous generation of ground-based detector. Although the next generation of satellite-borne instruments, like AGILE [1] and GLAST [2], will as well try to fill the observational gap from below, large difference in collection area, will give a privileged role to Cherenkov telescopes to study the phenomena in which high-sensitivity is required (low photon flux and rapidly variable phenomena). For this reason, the new generation of ground-based and satellite-borne experiments will play the role of complementary instruments in a vigorous physics campaign foreseen for the next decade. Among the new Cherenkov telescopes Major Atmospheric Gamma Imaging Cherenkov telescope (MAGIC) (Fig. 1) is the one designed to have the lowest energy threshold ($\sim$30 GeV), so it will be the first instrument exploring an interesting region of the observational energy gap. Several novel technologies have been used to build the worldwide largest air Cherenkov telescope and reach the lowest energy threshold. MAGIC has been built in the Canarian Island of La Palma (28.8N, 17.9W) at the *Roque de los Muchachos Observatory*, 2200 m above sea level. The key elements of the MAGIC telescope are described below.

2. The telescope frame

The 17 m diameter f/1 telescope frame is made of light weight carbon fiber tubes ($<$10 t). The construction of the foundation started in September 2001 and the telescope frame was completed in December 2001. The assembly of the frame took only 1 month, thanks to a construction based on the so-called *tube and knot* system of the company MERO. This system allowed the assembling of the entire frame without any welding. The light weight structure and the low inertia of the structure allows a fast slewing time in such a way that the telescope will be able to perform an early follow-up of a Gamma Ray Burst. With the engines at 70% full power, the telescope was able to move 180° (azimuth) in less than 30 s. The fast movement of such a large structure is very impressive.The tracking and slewing system have now been commissioned.

3. The reflector

The overall reflector shape is parabolic to minimize the time spread of the Cherenkov light

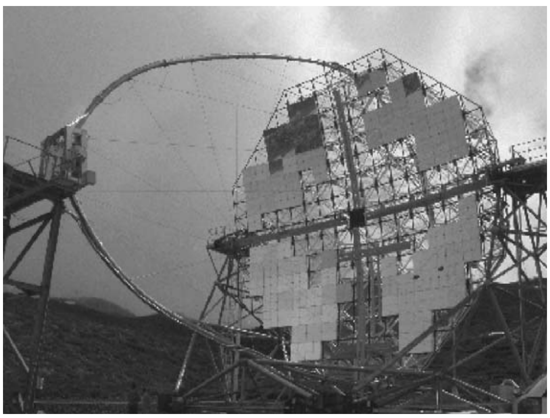

Fig. 1. View of the MAGIC telescope just after the camera installation December 2002, with 40% of the mirrors installed.

flashes in the camera plane. The preservation of the time structure of the Cherenkov flashes is important to increase the signal to noise ratio with respect to the night-sky background light. The parabolic dish is tessellated by 956 $0.5 \times 0.5\ \mathrm{m}^2$ covering a surface of $234\ \mathrm{m}^2$. Each mirror is sandwiched with the aluminum honeycomb on which a 5 mm plate of AlMgSi1.0 alloy is glued. The aluminum plate of each mirror tile, is diamond milled to achieve the spherical reflecting surface with the radius of curvature most adequate for its position on the paraboloid. A thin quartz layer protects the mirror surface from aging. Embedded in the honeycomb sandwich is a 0.3 mm Printed Circuit Board, of the same size of the mirror, which is used as an internal heater to prevent dew and ice deposition. The mirrors are grouped in panels of three or four, which can be oriented during the telescope operation through an active mirror control system to correct possible deformation of the telescope structure. After a careful pre-alignment of the mirrors in a panel, made during the panel assembling, the alignment of the mirrors in the telescope structure has been done by using an artificial light source at a distance of 920 m. In the latter procedure, the camera plane was moved 29 cm backward to focus the lamp light in the proper plane. The overall spot of the first $103\ \mathrm{m}^2$ aligned mirrors is roughly half pixel size FWHM $<0.05^\circ$. During the summer 2003 we plan to complete the mirror installation.

4. The camera

The MAGIC camera is a key element to improve the gamma sensitivity and gamma/hadron separation. The camera is 1.5 m in diameter, 450 kg weight and cover 4° of FOV. The inner hexagonal area is composed of 397 0.1° FOV PMTs of $1''$ diameter (ET 9116) surrounded by 180 0.2° FOV PMTs of $1.5''$ diameter (ET 9117). The typical time response FWHM is below 1 ns [3]. The photocathode QE is enhanced up to 30% and extended to UV by a special coating of the PM surface with Wavelength Shifter [4]. Each PM is connected to an ultrafast low-noise trans-impedance pre-amp, the 6-dynode HV system is zener stabilized with an active load. Dedicated light collectors have been designed to let the photon double-cross the PMT photocathodes for large acceptance angles. The HV regulation for each PMT fully covers the 0–2000 V range. The DC current and HV are read out for each pixel, multiplexed in groups of 96 and digitized by a 12 bit ADC. The temperature is controlled by a water-based cooling system with temperature/humidity sensors. The camera was completed in summer 2002 and after extensive tests and characterization was installed in November 2002 and has been commissioned in March 2003 after the winter break. First starlight using DC current readout was recorded on March 8th.

5. The read-out chain

PMT signals are amplified by ultrafast and low-noise trans-impedance pre-amplifier in the camera housing. The amplified analog signals are transmitted over 162 m long optical fibers using Vertical Cavity Surface Emitting Laser Drivers (VCSELs, $\lambda = 850$ nm). In the receiver board the signal is split, one branch is going to a discriminator with a software-adjustable threshold that generates a signal for the trigger system. The signal in the second branch is amplified, stretched to 6 ns FWHM and split into a high and low gain channel in order to increase the dynamic range. The high gain part is amplified to a factor of 10 while the low gain is delayed by 50 ns. If the signal is above a preset threshold the low-gain branch is combined with the high-gain one using a fast GaAs analog switch and digitised by the same FADC channel.

6. The trigger

The MAGIC trigger is a two-level advanced trigger system with programmable logic [5]. The first-level trigger (L1T) applies tight time coincidence and simple next-neighbour logic. The trigger is active in 19 hexagonal overlapping regions (trigger cells) of 36 pixels each, to cover 325 of the inner pixels of the camera. The second-level trigger (L2T) can be used to perform a rough analysis and apply topological constraints on the event images. It consists of a set of Look Up Tables, enabled from L1T, and acting on the 19 trigger cells with a tree-structured set of programmable fast memories. Using some topological constraints like a fast evaluation of the size of the image made by L2T [6], it is possible to reduce significantly the night sky background rate, allowing a reduction of the discriminators and gamma energy threshold.

7. The DAQ

Analog signals are continously digitized using an 8-bit 300 MHz FADC. The digitized samples are stored in 32 kbyte long ringbuffers. If a trigger signal arrives within less than 100 μs the position of the signal in the ringbuffer is determined and for each pixel 15 high gain plus 15 low gain samples are written to a 512 kbytes long FiFo buffer at a maximum rate of 80 Mbyte/s. The readout action of the ringbuffer results in a dead time of less than 1 μs. This corresponds to less than a 0.1% dead time at the design trigger rate of 1 kHz. The time and the trigger information for each event are recorded by dedicated digital modules which are read out together with the FADC modules. The readout is controlled by an FPGA (Xilinx) Chip on a PCI (MicroEnable) card. The FADC data stored in the FiFo buffers are read out with a rate of 4 bytes at 20 MHz. The data are saved to a RAID0 disk system at a rate of up to 20 Mbyte/s which generates up to 800 Gbyte raw data per night. During daytime, the data are transformed into a ROOT format and written to tape.

8. Calibration system

The MAGIC calibration system consists of a light pulser system and a continuous light source, both situated in the center of the mirror dish, a darkened, single photo-electron counting PMT ("blind pixel"), situated in the camera plane and a calibrated PIN-diode situated 1.5 m above the light pulsers. The pulsed light is emitted from very fast (3–4 ns FWHM) and powerful

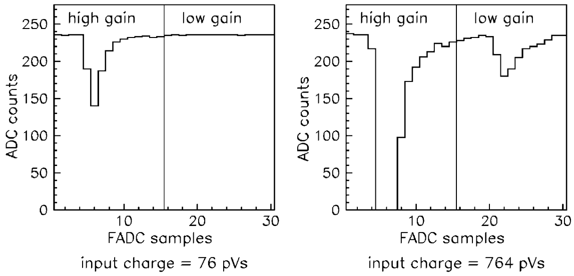

Fig. 2. Two test pulses with different input charge readed by the MAGIC DAQ. When a large signal makes a high-gain branch saturated, the low-gain side will appear 50 ns later (right plot).

(10^8–10^{10} photons/sr) light emitting diodes (LEDs) in three different wavelengths (370, 460 and 520 nm) and different intensities (up to 2000–3000 photo-electrons per pixel and pulse). It is thus able to calibrate the whole readout chain (from the PMT to the DAQ) (Fig. 2) with respect to wavelength and linearity. The continous light source consists of LEDs simulating the light of night sky at La Palma with differnt intensities. The absolute light flux incident on the camera is measured by three methods independently: via the blind pixel, the PIN-diode and using the traditional excess noise factor method which extracts the number of photo-electrons from the previously measured excess noise factor, the variance of the pedestal, the variance of the signal and the pedestal-corrected signal charge. The pedestals, on their turn, will be monitored regularly by measuring the variance of the pedestal charges. These variances can be cross-calibrated with the anode currents of each PMT using the continous light source and the fact that the currents are proportional to the square of the RMS noise in the PMT.

9. Conclusions and future plans

So far, all the new technical components implemented in this very large Cherenkov telescope behaved as expected. In the next few months we will make extensive tests of the apparatus with engineering and physics runs. We expect to start regular observations during this summer. It is our aim to consider MAGIC as the first element of an international observatory to study the deep universe with high energy gamma rays. Our proposal is to transform the MAGIC site, Roque de los Muchachos, into a European Cherenkov Observatory, dubbed ECO.

References

[1] M. Tavani, et al., SPIE 4851 (2003) 1151.
[2] N. Gehrels, et al., AIP Conf. Proc. 3 (2001) 558.
[3] A. Ostankov, et al., Nucl. Instr. and Meth. A 442 (2000) 117.
[4] D. Paneque, et al., Nucl. Instr. and Meth. A 504 (2003) 109.
[5] D. Bastieri, et al., Nucl. Instr. and Meth. A 461 (2001) 521.
[6] D. Corti, et al., The trigger system of the MAGIC telescope: on-line selection strategies for Cherenkov telescopes, Nucl. Instr. and Meth. A, (2004) these Proceedings.